

Vehicle parameter estimation using a model-based estimator

Matilde Paiano^a, Giulio Reina^a, Jose-Luis Blanco^b

^a*Dept. of Engineering for Innovation, University of Salento, Via Arnesano, 73100 Lecce, Italy*

^b*Dept. of Engineering, Universidad of Almería, 04120 Almería, Spain*

Abstract

In the last few years, many closed-loop control systems have been introduced in the automotive field to increase the level of safety and driving automation. For the integration of such systems, it is critical to estimate motion states and parameters of the vehicle that are not exactly known or that change over time. This paper presents a model-based observer to assess online key motion and mass properties. It uses common onboard sensors, i.e. a gyroscope and an accelerometer and it aims to work during normal vehicle maneuvers, i.e. turning motion and passing. First, basic lateral dynamics of the vehicle is discussed. Then, a parameter estimation framework is presented based on a Extended Kalman filter. Results are included to demonstrate the effectiveness of the estimation approach and its potential benefit towards the implementation of adaptive driving assistance systems or to automatically adjust the parameters of onboard controllers.

Keywords:

Vehicle state estimation, Extended Kalman filter, mass estimation, adaptive estimation, vehicle lateral dynamics

1. Introduction

The performance of driving assistance systems may be improved if the unknown parameters of the underlying vehicle model can be measured and updated. Weight of the vehicle, road adhesion, drag coefficient and tire cornering stiffness are examples of unknown parameters. Specifically, the mass of a vehicle plays an important role in terms of acceleration/braking, handling and comfort performance. However, it is subject to variations during operating conditions. For heavy duty vehicles, the weight can vary as much as 400% according to the payload. Anti-lock Braking System (ABS), Electronic Stability Program (ESP), and Adaptive Cruise Control (ACC) are all examples of controllers that relies on the accurate value of the vehicle mass for proper operation. Current implementations work with the assumption of a maximum payload to provide passengers with the highest level of comfort and safety independently of the load conditions. Therefore, the introduction of automatic load detection systems will be the basis for some more vehicle improvements. As soon as onboard controllers can incorporate information about the actual vehicle weight in their response, this will enable them to provide even more efficient comfort and support for drivers. Therefore, they may achieve better results by taking the actual vehicle weight into account. The paper is organized as follows. Section 2 surveys related research pointing out the novel contributions of the proposed approach. In Section 3, basic concepts of lateral vehicle dynamics are recalled that serve as a basis for the model-based observer described in Section 4. The proposed method recursively updates the vehicle mass providing flexibility to the observer. The technique is studied in a sequence of simulations, as detailed in Section 5,

26 attesting to the feasibility of the proposed approach. Finally, Section ??
27 concludes the paper.

28 **2. Related Work**

29 Vehicle parameter estimation is a critical issue connected with the inte-
30 gration of onboard control systems, especially when these parameters change
31 over time or they are difficult to measure directly [1]. Therefore, the availabil-
32 ity of an online estimation method for the vehicle's weight would be valuable
33 as it greatly affects its behaviour in terms of longitudinal, lateral and vertical
34 dynamics. In addition, as the level of driving automation increases, there are
35 more control modules that may benefit from on-line estimation of the vehi-
36 cle's load, including longitudinal control of platoons of vehicles [2], emission
37 reduction and transmission control [3].

38 In general, the methods proposed in the literature can be classified in two
39 broad families: sensor-based and model-based methods. In sensor-based
40 methods, an additional dedicated sensor is employed. As an example, the
41 vehicle's weight can be estimated by monitoring the suspension deflection us-
42 ing strain gages [4] or an electro-magnetic sensor [5]. Recently, Continental
43 has announced a future generation of sensors, which will be fitted directly
44 underneath the tread of the tire to measure the total weight of the vehicle [6].
45 As the contact patch of the tire increases with the vertical load, by detecting
46 the size of the contact area, it will be possible to infer information about the
47 vehicle's weight.

48 In contrast, model-based (or indirect) methods use a model of the vehicle,
49 software algorithms and existing sensors (different from direct mass sensors)

50 to estimate the unknown parameter. They represent a promising solution in
51 terms of cost-effectiveness (no extra hardware). Most of the research in this
52 field focuses on the longitudinal dynamic problem. Examples of adaptive
53 controllers for vehicle speed control can be found in [7], [8]. Simultaneous
54 estimation of vehicle mass and road grade has been studied by many. For
55 example, an adaptive control scheme for longitudinal control of heavy-duty
56 vehicles is proposed in [9], whereas [10] propose the use of Recursive Least
57 Squares (RLS) with multiple forgetting factors. An EKF approach is pro-
58 posed in [11] using two possible measurement configurations: the first one
59 using only the vehicle speed and a second one in conjunction with an addi-
60 tional longitudinal accelerometer. The advantages of using an accelerometer
61 are also shown in [12] where a method to estimate vehicle mass and road
62 grade using an EKF is presented. An active estimator is proposed in [13] to
63 enhance parameter identifiability through the use of an EKF for parameter
64 estimation and model predictive control to control vehicle speed.

65 A body of research also deals with vertical dynamics for vehicle mass esti-
66 mation. Often, these methods assume that the terrain profile is known or
67 estimated [14], [15], [16], [17]. In [18] the vertical response is analyzed in the
68 frequency domain to reveal important resonance frequencies related to the
69 value of the sprung mass.

70 Another strand of the research on mass estimation focuses on powertrain dy-
71 namics. For example, in [19] the mass of a truck is estimated by measuring
72 vehicle speed and engine torque and angular velocity during acceleration and
73 gear shifting stages, resulting in an accuracy of 10%.

74 In this work, an adaptive observer for automatic weight estimation is pre-

75 sented based on the lateral dynamic model of the vehicle, which represents a
 76 novel contribution to the literature. An EKF formulation is proposed where
 77 the varying parameter is included in the state vector and continuously up-
 78 dated using current sensory data. This formulation has general value and it
 79 may be used to track any other time-varying parameter provided that the
 80 observability condition is satisfied.

81 3. Vehicle model

The lateral behaviour is an important aspect in vehicle design, as it directly affects handling and comfort properties. Figure 1 shows the two degree-of-freedom model used in this research commonly known as the “bicycle” or “single track” model that holds under the following simplifications [20]: no weight transfer, constant vehicles longitudinal velocity u , equal internal and external dynamics so that tires of the same axle can be collapsed, linear range of the tires, rear-wheel drive, negligible motion resistance, and small angle approximation. The two degrees of freedom are the vehicle lateral velocity v and yaw rate r . The equations of motion for the single-track model are given by:

$$\dot{v} = -\left(\frac{C_F+C_R}{Mu}\right)v - \left(\frac{C_Fa-C_Rb}{Mu} + u\right)r + \frac{C_F\delta}{M} \quad (1)$$

$$\dot{r} = -\left(\frac{C_Fa+C_Rb}{Iu}\right)v - \left(\frac{C_Fa^2+C_Rb^2}{Iu}\right)r + \frac{C_Fa\delta}{I}$$

where M and I are the mass and the rotational inertia of the vehicle, δ is the front steer angle, a and b are the distance of the centre of gravity G from the front and rear axle, respectively, and C_F and C_R are the front and rear tire cornering stiffness. In the study of lateral dynamics it is often useful to

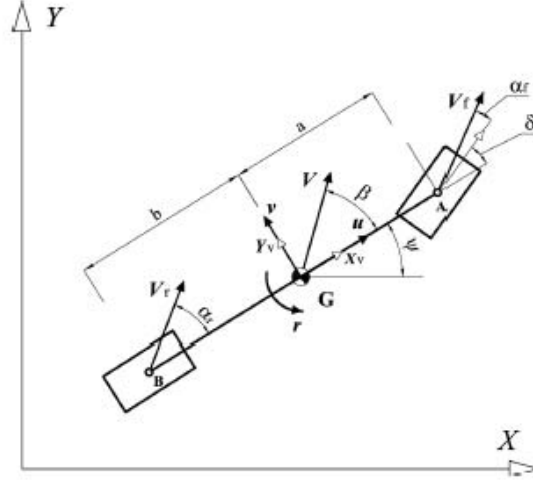


Figure 1: Lateral vehicle dynamics

refer to the sideslip angle β , defined as the angle between the vector velocity pertaining to the centre of mass and the longitudinal axis of the vehicle X_V :

$$\beta = \arctan \frac{v}{u} \quad (2)$$

Note that in conventional models, the mass is usually treated as a fixed parameter that typically refers to the maximum load condition. In this study, M is treated as a time-varying parameter. As a consequence, Eq. (1) expresses a non-linear relationship between v , r , and M .

The method proposed in this paper for online mass estimation is based on the use of a vertical gyroscope and a lateral accelerometer. Considering that both sensors are generally available onboard via the ESP system, this approach results particularly attractive in terms of cost-effectiveness, requiring only additional software efforts.

The gyro signal r_g is generally subject to an offset error and needs to be mod-

eled [21]. A good working approximation of gyro measurement is $r_g = r + b_g$. The relationship between accelerometer's measurement and the state variables is $a_y = \dot{v} + ur$.

The state evolution of the nonlinear system can be represented in compact matrix form as

$$\dot{x}(t) = f(x(t), \delta(t)) \quad (3)$$

where x is the state vector and $f(\cdot)$ is the state evolution function. x is given by

$$x = [v, r, \dot{v}, \dot{r}, b_g, M]^T \quad (4)$$

Similarly, if the measurement vector z is introduced

$$z = \begin{bmatrix} r_g \\ a_y \end{bmatrix} \quad (5)$$

a measurement equation can be drawn in compact matrix form as

$$z(t) = h(x(t)) \quad (6)$$

82 In summary, Eq. (3) and Eq. (6) can serve as the basis for non-linear
 83 estimation methods. In the context of this problem, an extended Kalman
 84 filter or EKF is found to be a good solution, as explained in the next section.

85 4. Vehicle estimation

86 It is not always possible to directly measure all states describing the ve-
 87 hicle's dynamic behavior because of technical and/or economic reasons. In
 88 addition, some of the model parameters may be uncertain or change over
 89 time. Nevertheless state/parameter estimation may be inferred by deriva-
 90 tion using other available sensors through the use of observers or virtual

91 sensors. Observation means the extraction of information of a given variable
92 of interest that is not directly measurable by using only available sensor data.
93 The idea behind the proposed research is to implement a model of the real
94 system in an onboard computer that runs in parallel with the system itself
95 providing estimation of a given set of states or variables of interest. One
96 challenge is that the system to be observed is usually excited by a stochastic
97 noise, due for example to imperfections in modeling the system. In addition,
98 sensor measurements may be biased and affected by their own stochastic
99 noise. Therefore, a stochastic closed-loop observer is necessary. One com-
100 mon solution is the Kalman filter whose scope in this study is extended to
101 mass estimation as well by incorporating M in the state vector. The pro-
102 posed framework is of general value and may be easily modified to track
103 other time-varying parameters. In the proposed embodiment, explained in
104 the block diagram of Figure 2, the Kalman filter-based observer runs in
105 parallel with the system. Driver commands, i.e. the steer angle and the
106 longitudinal speed (δ, u) and measurements of vehicles's response (r_g, a_y) are
107 fed into the estimator that recursively estimates the states (i.e., β and r) and
108 parameters (i.e., M) of the system online during normal vehicle manoeuver-
109 ing. Additionally, the estimator provides estimate of gyroscope's bias that
110 can be used for on-line sensor calibration.

111 *4.1. Model-based Extended Kalman observer*

The Kalman filter addresses the general problem of estimating the state of a discrete-time controlled process that is governed by a difference equation (i.e., Eq. (3)) with a measurement (i.e., Eq. (6)). The first step is to express

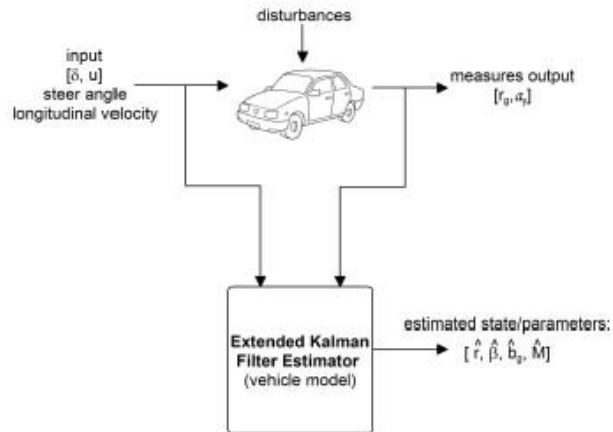


Figure 2: Block diagram of the proposed approach for state/parameter estimation using an EKF running in parallel

the non-linear model in a stochastic discrete-time state-space representation

$$x_k = f(x_{k-1}, \delta_k) + w_{k-1} \quad (7)$$

$$z_k = h(x_k) + v_k \quad (8)$$

where $x_k = [v_k, r_k, \dot{v}_k, \dot{r}_k, b_{g,k}, M_k]^T$ is the state vector at time k , δ_k is the input vector at time k , and z_k is the observation sampled at time k . If the system is discretised using the first-order Euler approximation with sampling

time Δt , $f(\cdot)$ becomes

$$\begin{aligned}
f_1 : v_k &= v_{k-1} + \dot{v}_{k-1} \Delta t \\
f_2 : r_k &= r_{k-1} + \dot{r}_{k-1} \Delta t \\
f_3 : \dot{v}_k &= - \left(\frac{C_F + C_R}{M_{k-1} u} \right) v_{k-1} - \left(\frac{C_F a - C_R b}{M_{k-1} u} + u \right) r_{k-1} + \frac{C_F \delta_k}{M_{k-1}} \\
f_4 : \dot{r}_k &= - \left(\frac{C_F a + C_R b}{M_{k-1} a b u} \right) v_{k-1} - \left(\frac{C_F a^2 + C_R b^2}{M_{k-1} a b u} \right) r_{k-1} + \frac{C_F a \delta_k}{M_{k-1} a b} \\
f_5 : b_{g,k} &= b_{g,k-1} \\
f_6 : M_k &= M_{k-1}
\end{aligned} \tag{9}$$

whereas $h(\cdot)$ can be obtained as

$$\begin{aligned}
h_1 : r_{g,k} &= r_k \\
h_2 : a_{y,k} &= \dot{v}_k + u r_k
\end{aligned} \tag{10}$$

The process disturbance and the measurement noise, w_k and v_k , respectively, are assumed to be Gaussian, temporally independent of each other, and white, Q and R being the process and measurement noise covariance, respectively.

The Kalman filtering estimation operates through the prediction-correction cycle expressed by an *a priori* estimation:

$$\begin{aligned}
\hat{x}_k^- &= f(\hat{x}_{k-1}, \delta_k) \\
P_k^- &= A_k P_{k-1} A_k^T + Q
\end{aligned} \tag{11}$$

and a measurement update, which is only performed when the measurements are available, providing an *a posteriori* estimation:

$$\begin{aligned}
K_k &= P_k^- H_k^T (H_k P_k^- H_k^T + R)^{-1} \\
\hat{x}_k &= \hat{x}_k^- + K_k (z_k - H_k \hat{x}_k^-) \\
P_k &= (I - K_k H_k) P_k^-
\end{aligned} \tag{12}$$

where \hat{x}_k^- is the predicted state vector, P_k^- is the variance matrix for \hat{x}_k^- , K_k is the gain matrix, \hat{x}_k is the updated state vector, and P_k is the updated error covariance estimate. The prediction equations are responsible for projecting forward in time the current state and error covariance estimates to obtain the *a priori* estimate for the next time step. The correction equations are responsible for the feedback, i.e. for incorporating a new measurement into the *a priori* estimate to obtain an improved *a posteriori* estimate.

In these equations, A_k and H_k are, respectively, the process and measurement Jacobian (matrix of partial derivatives of f (h , respectively) with respect to x) at step k of the nonlinear equations around the estimated state

$$A_k = \begin{bmatrix} 1 & 0 & \Delta t & 0 & 0 & 0 \\ 0 & 1 & 0 & \Delta t & 0 & 0 \\ A_{31} & A_{32} & 0 & 0 & 0 & A_{36} \\ A_{41} & A_{42} & 0 & 0 & 0 & A_{46} \\ 0 & 0 & 0 & 0 & 1 & 0 \\ 0 & 0 & 0 & 0 & 0 & 1 \end{bmatrix} \quad (13)$$

$$H_k = \begin{bmatrix} 0 & 1 & 0 & 0 & 1 & 0 \\ 0 & u & 1 & 0 & 0 & 0 \end{bmatrix} \quad (14)$$

112 Please refer to the Appendix for the expression of the terms $A_{i,j}$ in A_k .

113 Finally, one should note that the measurement noise covariance R is used
 114 to define the error of the sensor readings. Table 1 collects the sensor noise
 115 and bias used in this research that can be found on the sensor specification
 116 sheet or from observing static data from the sensor.

Table 1: Sensor technical details

	Gyroscope	Accelerometer
Sensor noise (1σ)	1 deg/s	0.5 m/s^2
Output rate	200 Hz	200 Hz
Offset	0.1 deg/s	-

117 4.2. *Observability test for non-linear system*

An important aspect of the state estimation problem is the observability. A system is said to be *observable* at a time step k_0 if, for a state $x(k_0)$ at that time, there is a finite $k_1 > k_0$ such that knowledge of the output z from k_0 to k_1 is sufficient to determine state k_0 [15].

The time derivative of measurement z is:

$$\frac{dz}{dt} = \frac{\partial h}{\partial x} \frac{dx}{dt} = \frac{\partial h}{\partial x} f(x) \quad (15)$$

118 Higher derivatives of z can be written compactly by introducing the operator
119 L_f (*Lie derivative*).

120 $L_f[h] = \frac{\partial h}{\partial x} f(x) =$ time derivative of h along the system trajectory x .

121 $\Rightarrow \frac{d^2 z}{dt^2} = \frac{\partial}{\partial x} \left(\frac{\partial h}{\partial x} f(x) \right) f(x) = L_f[L_f[h]] = L_f^2[h]$

Therefore:

$$\frac{d^k z}{dt^k} = L_f^k[h] \quad (16)$$

A system with state vector x of dimension n is *locally observable* at x_0 if the observability matrix:

$$O(x_0, \delta) = [dL_f^0[h] = dh, dL_f^1[h], \dots, dL_f^i[h], \dots, dL_f^{n-1}[h]]^T \quad (17)$$

122 has row rank n (i.e. n linearly independent rows).

123 In our case the observability matrix has dimension $n = 6$. To calculate the
124 analytical expression of $O(x_0, \delta)$ the function `diff(.)` of the Matlab Symbolic
125 tool is used. $O(x_0, \delta)$ resulted in full rank, therefore the system is locally
126 observable.

127 5. Results

This section presents simulation results to show the effectiveness of the proposed approach for on-line mass estimation. In all simulations, the parameters of a typical passenger car are used (see Table 2). A common passing or double lane-change manoeuvre is considered, where the driver quickly swerves into the passing lane to avoid a slower car or an obstacle and then immediately swerves back to avoid oncoming traffic. Passing can be expressed by a sine function for steering input

$$\begin{aligned}\delta(t) &= \delta_0 \sin \omega t \\ \omega &= \frac{2\pi L}{u}\end{aligned}\tag{18}$$

128 where L is the moving length during the lane change and u is the forward
129 velocity of the vehicle. For a speed of 80 km/h, $L = 33\text{m}$, and steering
130 wheel angle comprised between -80 and 80 degrees (steering ratio $\tau = 1/20$),
131 the corresponding driver command and illustrative path are shown in Figure
132 3. The lateral behaviour of the vehicle is simulated by discretizing Eq. (3)
133 and Eq. (6) with process and sensor noise. The sensor measurements are
134 corrupted with random noise of the standard deviation as claimed in the
135 specification of the sensor (see Table 1). Additionally, a bias that is within the
136 normal sensor's specification is added to the gyroscope. The measurements

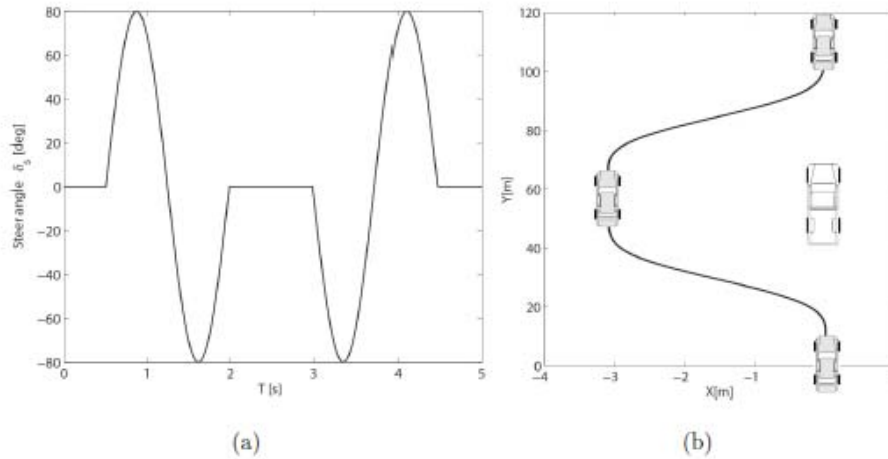


Figure 3: Double lane change: (a) steering wheel angle, (b) path followed by the vehicle.

137 are corrupted in order to provide realistic sensory input to the model-based
 138 observer. The correct process noise is given to the estimator.

139 5.1. Parameter sensitivity

140 First, a simulation is performed to show the effects of incorrect model
 141 parameters (i.e., vehicle load) on a conventional observer based on a “static”
 142 model with fixed parameters, i.e. without on-line mass estimation. The
 143 estimator model is given an incorrect value of mass increased of 20% with
 144 respect to the actual value ($M=1400$ kg). Results are shown in Figure 4(a) in
 145 terms of simulated and estimated vehicle states r and β and they reveal how
 146 model parameter error leads to biased estimations of the states. One way
 147 to check the observer accuracy is to look at the residuals, i.e., the difference
 148 between the actual and the estimated measurements. The residuals for a
 149 correct observer should be white noise with zero mean. Conversely, in Figure
 150 4(b) residuals for the rate of turn and lateral acceleration, as obtained from

Table 2: Parameters of the passenger car used in the simulations, please refer to Figure 1 for more details

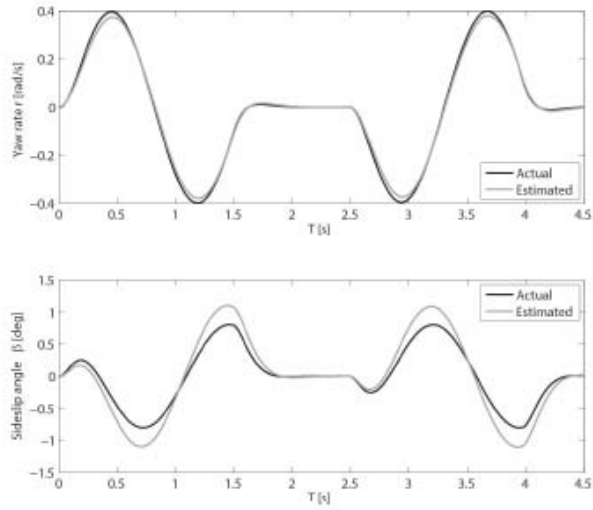
a	1.108 m
b	1.492 m
C_F	117,240 N/rad
C_R	142,720 N/rad
M	1400 – 1683* kg
I	$M \cdot a \cdot b$

* The first and second value refer to the empty vehicle and maximum load, respectively

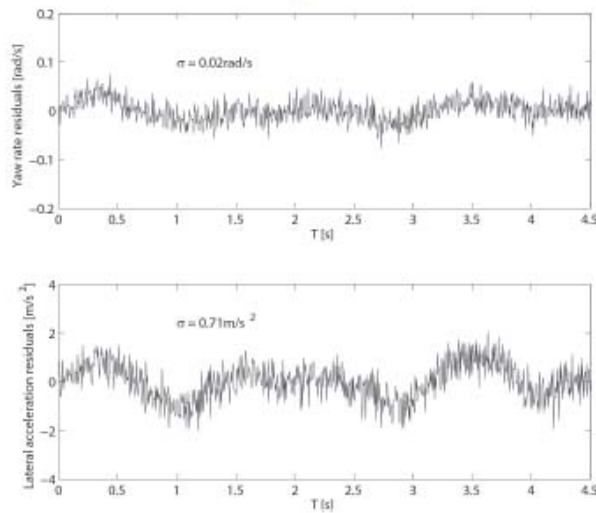
151 the observer with incorrect parameter, show a definite shape (or correlation).
 152 The same manoeuver was repeated using the correct value of the vehicle mass
 153 in the estimator. Results are collected in Figure 5(a), demonstrating that
 154 estimation is very accurate with correct parameters even in the presence of
 155 noisy and biased sensor measurements. This is also confirmed when looking
 156 at the residuals of measurements that appear approximately as a zero mean
 157 white noise (Figure 5(b)).

158 5.2. Adaptive estimation

Results presented in the previous section showed that the availability of an adaptive estimator for on-line mass estimation would be of great value to enhance the performance of on-board control systems by continuously updating the parameters of the vehicle model. A passing manoeuver simulation was performed using the adaptive observer proposed in this research.

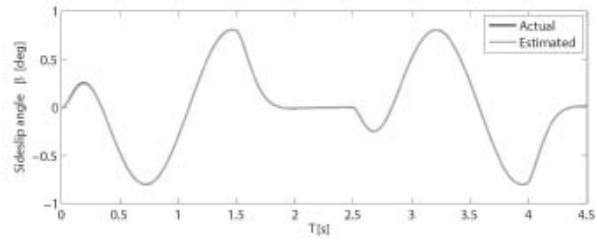
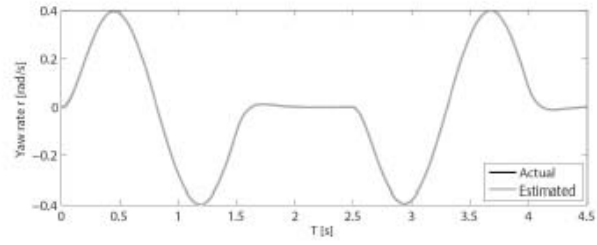


(a)

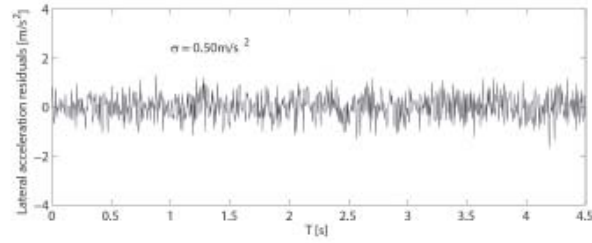
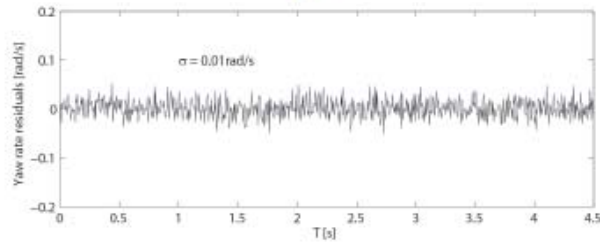


(b)

Figure 4: (a) State estimation and (b) residuals as obtained from a “static” estimator using incorrect parameters in the vehicle model for a double lane-change manoeuvre



(a)



(b)

Figure 5: (a) State estimation and (b) residuals as obtained from a “static” estimator using exact parameters in the vehicle model for a double lane-change manoeuvre

Initially, the observer is given an erroneous value of the vehicle mass corresponding to the maximum load condition, i.e., $M_0 = 1683$ kg. Estimation of states r , β and M as obtained from the observer is shown in Figure 6. In detail, the lower plot of Figure 6 shows the recursive mass estimation denoted by a solid grey line. The module corrects the parameter towards its actual value $M = 1400$ kg (denoted by a black dashed line), after an approximately 1 second adaptation window (the time required to reach 90% of the actual value is 0.39 seconds). As the system adjusts to the actual vehicle mass, the observer response becomes more accurate and the discrepancy of the state estimates r and β with respect to the actual values decreases, as shown in the upper and middle plot of Figure 6, respectively.

Uncertainty in the estimation, expressed as standard deviation (3σ), is also shown denoted by a grey shaded area along the corresponding curves. In detail, the variance of r coincides with the term $P_k(2, 2)$ of the error covariance matrix. The variance of β , P_k^β , can be obtained by applying the law of uncertainty propagation:

$$P_k^\beta = J_k P_k^v J_k^T \quad (19)$$

Where J_k is the Jacobian matrix and P_k^v is the covariance of the variables which β depends on, i.e. the state v .

From Eq. (2), it results:

$$J_k = \begin{pmatrix} \frac{1}{u(1+(\frac{v}{u})^2)} & 0 \end{pmatrix} \quad (20)$$

$$P_k^\beta = J_k \begin{pmatrix} P_k(1, 1) & 0 \\ 0 & 0 \end{pmatrix} J_k^T \quad (21)$$

159 As seen in Figure 6, the estimation uncertainty tends to decrease as the
 160 accuracy in the mass estimation improves.

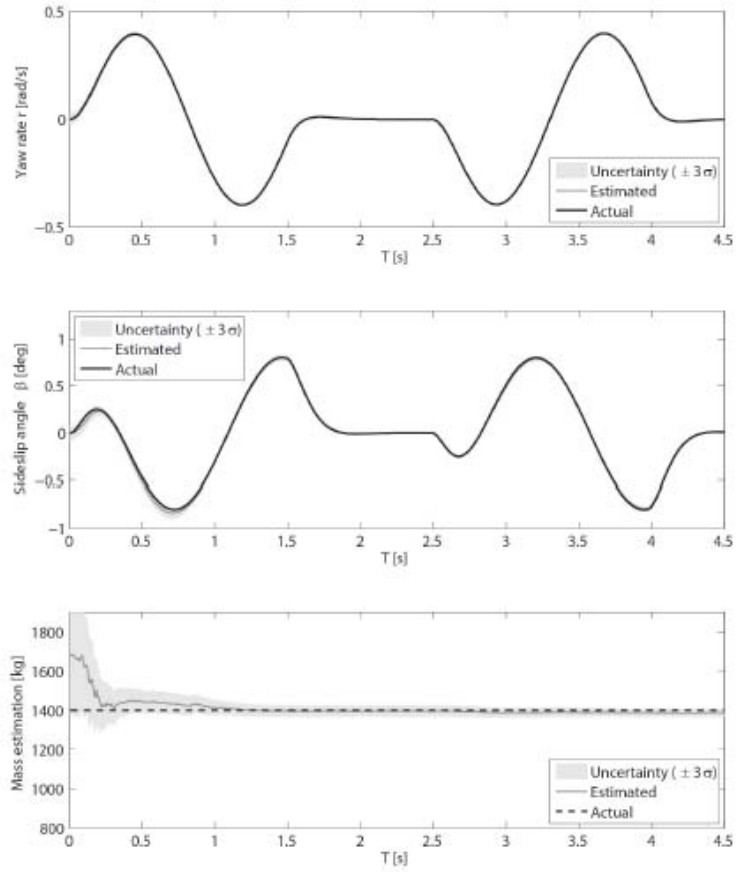


Figure 6: Results obtained from the proposed adaptive observer for a double lane-change manoeuvre. The accuracy in state estimation improves as the mass estimation tends to the actual value.

161 Figure 7 shows a comparison of the noisy measurements given in input to the
162 system (denoted with a solid grey line) with the output obtained from the
163 estimator (marked by a solid black line) in terms of yaw rate r and lateral
164 acceleration a_y , respectively. It is apparent the good work of the adaptive
165 estimator in “cleaning” the sensor data (upper and middle plot of Figure 6).
166 The gyroscope measurement is also successfully updated in a few seconds,
167 as shown in the lower plot of Figure 7. Again, the uncertainty in the bias
168 estimation is denoted by a grey shaded area along the estimation curve.

169 5.3. System performance

170 In order to evaluate how the adaptive observer behaves under different op-
171 erating conditions various step-steer simulations are performed by changing
172 forward speed u and steer angle δ .

173 Add results

174

175 Another important aspect is the system sensitivity, i.e. the minimum
176 detectable change in the vehicle load. A double lane-change manoeuvre with
177 travel speed of xx and steer angle amplitude yy is simulated by setting the
178 initial value of the vehicle mass 5% lower than the actual value, i.e. $M_0 =$
179 1330kg. Results are shown in Figure 8 in terms of estimation of state M and
180 its associated uncertainty.

181 The system responds well even in case of small changes in the vehicle load.
182 One additional advantage is that, the observer does not require any reset
183 procedure or learning stage that can be typically time consuming and difficult
184 to perform.

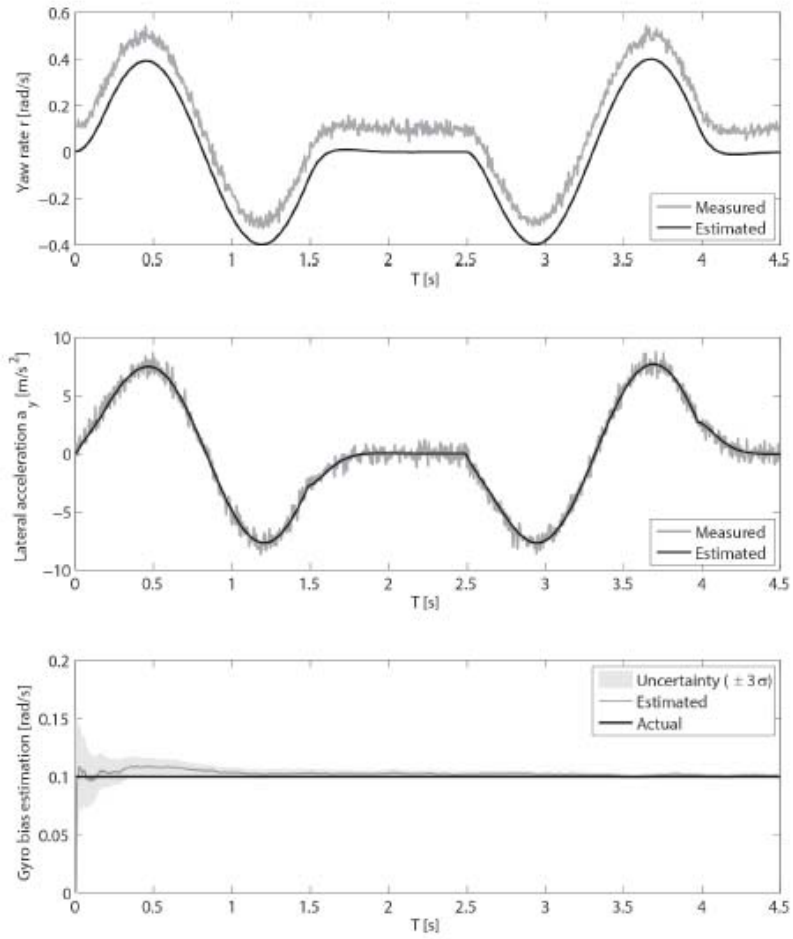


Figure 7: Results obtained from the proposed adaptive observer for a double lane-change manoeuvre. The noisy measurements are smoothed by the filter and the gyroscope bias is successfully updated on-line.

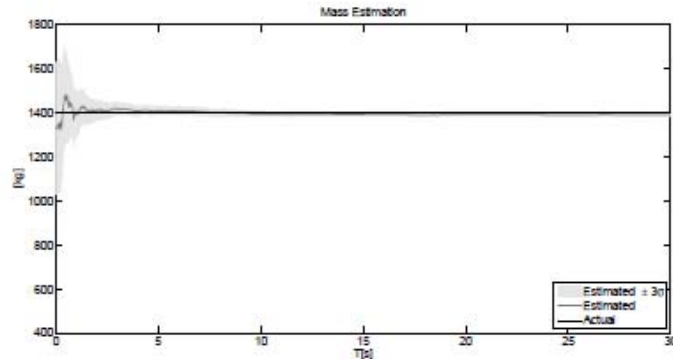


Figure 8: Minimum change of M...rifare figura con ingresso corretto

185 6. Conclusions

186 A model-based estimator for estimating vehicle's mass during normal
 187 driving and using only standard sensors was presented. The algorithm is
 188 based on a Extended Kalman filter to give robust and accurate estimates of
 189 the vehicle load and, at the same time, to allow abrupt changes to be tracked
 190 quickly. Results obtained from extensive simulation tests were presented to
 191 validate the proposed approach, using common manoeuvres (i.e., step-steer
 192 and double lane-change) and varying operating conditions (i.e., varying travel
 193 speed and steer angle). The sensitivity of the system was also studied. Es-
 194 pecially, variations in the vehicle load can be detected quite accurately. The
 195 proposed approach could be useful to implement warning and safety systems
 196 and for accurate estimation of the vehicle states as possible input to onboard
 197 control systems.

198 A possible limitation of this approach is that it may perform poorly un-
 199 der low excitation conditions. Before implementation, the system should be

200 evaluated in field tests on a long-term basis.

201 Acknowledgments

202 The financial support of the ERA-NET ICT-AGRI2 through the grant S3-
 203 CAV is gratefully acknowledged. This work has funded by the National Plan
 204 Project DPI2014-56364-C2-1-R.

205 Appendix

$$\begin{aligned}
 A_{31} &= -\frac{C_F + C_R}{M_{k-1}u} \\
 A_{32} &= -\left(\frac{C_F a - C_R b}{M_{k-1}u} + u\right) \\
 A_{41} &= -\frac{C_F a + C_R b}{M_{k-1}abu} \\
 A_{42} &= -\frac{C_F a^2 + C_R b^2}{M_{k-1}abu} \\
 A_{36} &= \frac{C_F + C_R}{M_{k-1}^2 u} \hat{v}_{k-1} + \frac{C_F a - C_R b}{M_{k-1}^2 u} \hat{r}_{k-1} - \frac{C_F \delta_k}{M_{k-1}^2} \\
 A_{46} &= \frac{C_F a - C_R b}{M_{k-1}^2 abu} \hat{v}_{k-1} - \frac{C_F a^2 + C_R b^2}{M_{k-1}^2 abu} \hat{r}_{k-1} - \frac{C_F \delta_k}{M_{k-1}^2 b}
 \end{aligned} \tag{22}$$

206

207 References

- 208 [1] G. Reina, A. Messina, A. Gentile, Tyre pressure monitoring using a dy-
 209 namical model-based estimator, *Vehicle System Dynamics* 53(4) (2015)
 210 568–586.
- 211 [2] H. Bae, J. Gerdes, Parameter estimation and command modification for
 212 longitudinal control of heavy vehicles, in: *Proc. of International Sym-
 213 posium on Advanced Vehicle Control*, 2000.

- 214 [3] U. Kiencke, L. Nielson, *Automotive Control Systems*, Springer, New
215 York, 2000.
- 216 [4] S. Yang, T. Liu, Y. Cheng, Automatic measurement of payload for heavy
217 vehicles using strain gages, *Measurement* 41 (2008) 491–502.
- 218 [5] K. Nishitani, Electromagnetic-type load weighing apparatus, United
219 States Patent 5,243,146.
- 220 [6] Continental-corporation, Intelligent tire sensors from con-
221 tinental will detect vehicle weight, On the WWW, uRL
222 www.continental-corporation.com/www/pressportal_com_en/themes/press_releases/
223 (January 2013).
- 224 [7] M. Liubakka, D. Rhode, J. Winkelman, P. Kokotovic, Adaptive auto-
225 motive speed control, *IEEE Transactions on Automatic Control* 38(7)
226 (1993) 146–156.
- 227 [8] R. Rajamani, *Vehicle Dynamics and Control*, Springer, 2012.
- 228 [9] M. Druzhinina, A. Stefanopoulou, L. Moklegaard, Adaptive contin-
229 uously variable compression braking control for heavy-duty vehicles,
230 *ASME Dynamic Systems, Measurement and Control* 124(3) (2002) 406–
231 414.
- 232 [10] A. Vahidi, A. Stefanopoulou, H. Peng, Recursive least squares with for-
233 getting for on-line estimation of vehicle mass and road grade: theory
234 and experiments, *Vehicle System Dynamics* 43(1) (2005) 31–55.

- 235 [11] P. Lingman, B. Schmidtbauer, Road slope and vehicle mass estimation
236 using kalman filtering, in: Proceedings of the 17th IAVSD symposium,
237 2001.
- 238 [12] J. Holm, Vehicle mass and road grade estimation using kalman filter,
239 Ph.D. thesis, Linkoping University, Sweden (2011).
- 240 [13] V. Winstead, I. V. Kolmanovsky, Estimation of road grade and vehicle
241 mass via model predictive control, in: Proceedings of IEEE Conference
242 on Control Applications, 2005.
- 243 [14] C. Kim, P. I. RO, Reduced-order modelling and parameter estimation
244 for a quarter-car suspension system, *Journal of Automobile Engineering*
245 214 (2000) 851–864.
- 246 [15] M. Doumiati, A. Charara, A. Vicotrino, D. Lechner, *Vehicle Dynamics*
247 *Estimation using Kalamn Filtering*, Wiley, 2013.
- 248 [16] A. E. Blanchard, C. Sandu, A polynomial chaos-based kalman filter
249 approach for parameter estimation of mechanical systems, *Journal of*
250 *Dynamic Systems, Measurement and Control* 132 (2010) 061404 (18
251 pp.).
- 252 [17] B. L. Pence, H. K. Fathy, J. L. Stein, Recursive estimation for reduced-
253 order state-space models using polynomial chaos theory applied to vehi-
254 cle mass estimation, *IEEE Transactions on Control Systems Technology*
255 22(1) (2014) 224–229.
- 256 [18] R. Tal, S. Elad, Method for determining weight of a vehicle in motion,
257 United States Patent 034570.

- 258 [19] E. Ritzen, Adaptive vehicle weight estimation, Ph.D. thesis, Linköping
259 University, Sweden (1998).
- 260 [20] R. Jazar, Vehicle Dynamics, Springer-Verlag, New York, NY, USA, 2014.
- 261 [21] N. Persson, F. Gustafsson, M. Drevö, Indirect tire pressure monitoring
262 using sensor fusion, in: SAE paper, 2002, pp. 1–6, paper number 2002-
263 01-1250.